Multi-plateau force-extension curves of long double-stranded DNA.

Alexander Y. Afanasyev[†] and Alexey V. Onufriev[*,‡,¶]

†*Department of Biomedical Engineering and Mechanics, Virginia Tech, Blacksburg, VA 24061, USA*

‡*Departments of Computer Science and Physics, Virginia Tech, Blacksburg, VA 24061, USA*

¶*Center for Soft Matter and Biological Physics, Virginia Tech, Blacksburg, VA 24061, USA*

E-mail: alexey@cs.vt.edu

Abstract

When highly stretched, double-stranded DNA exhibits a plateau region in its force-extension curve. Here, we investigate the possibility of multiple distinct plateau regions in the force-extension curves of non-supercoiled double-stranded DNA under physiologically relevant conditions, and explore how their existence and properties are related to the DNA sequence. Using a bead-spring coarse-grained dynamic model based on a non-convex potential, we predict that a long non-supercoiled double-stranded DNA fragment made up of several segments with substantially different plateau force values for each individual segment will exhibit multiple distinct plateau regions in the force-extension curve under physiological solvent conditions at room temperature. The order of the segments does not affect the force-extension curve or the distribution of conformational states. As an example, a double-stranded DNA fragment consisting of two equal-length segments with two different plateau force values (poly(dA-dT)-poly(dG-dC) fragment) is predicted to exhibit two distinct plateau regions in its force-extension

curve; a fragment consisting of three almost equal-length segments having three different plateau force values (poly(dA-dT)-torsionally constrained DNA-poly(dG-dC) fragment) is predicted to have three distinct plateau regions. The formation of mixed states of slightly and highly stretched DNA, co-existing with macroscopically distinct phases in several segments in the plateau regions, is also predicted. We speculate that the distinct structural states of stretched double-stranded DNA may have functional importance. For example, these can modulate, in a sequence-dependent manner, the rate of double-stranded DNA processing by key cellular machines.

1 Introduction

A double-stranded (ds) DNA molecule is constantly subjected to different loading conditions in living cells.[1–3] Knowledge of the mechanical properties of the molecule[4] is important to understand many key cellular processes.[5–8] A widely used experimental technique employed to explore the mechanics of the polymer, the single-molecule stretching with optical or magnetic tweezers,[6,9–11] reveals a peculiar plateau region in force-extension curves of dsDNA.[9,12–14]

To describe the plateau region, a variety of theoretical models.[15–24] were proposed; a number of coarse-grained or fully atomistic molecular dynamics (MD) simulation studies revealed various aspects of the plateau region, including possible structural forms of the dsDNA under these conditions.[25–35] Sequence-dependence of dsDNA mechanical properties were addressed in a number of studies, see e.g.[36–39] In particular, the plateau force values in the force-extension curves of DNA, were found to be sequence-dependent,[27] in agreement with experiments.[21,40] It was computationally shown[25] that once the DNA is stretched beyond a certain threshold – the beginning of the plateau region – the extension of the polymer is no longer uniform along the chain: chain fragments separate into slightly stretched ones and highly stretched ones. The relative fraction of the slightly stretched fragments decreases linearly with the overall relative extension, reaching zero at the end of the plateau region. The slightly and highly stretched fragments are distributed randomly along the chain, without

forming macroscopically distinct phases.[35]

To date, the absolute majority of experimental (and theoretical) works in the field focused on the single plateau region in the force-extension curve of dsDNA. There are a limited number of experimental studies,[12,18,41] in which two plateau regions in the force-extension curves of dsDNA were experimentally observed. As an example, two plateau regions were experimentally seen in the force-extension curves of dsDNA in 5 M Betaine solution[12] i.e., in a distinctly non-aqueous solvent. Combining two segments with very different AT content can lead to two distinct plateaux that were predicted by a multi-state model of DNA stretching in Ref. 42. In another experimental work,[18] two plateau regions were seen for supercoiled DNA with 500 mM of added NaCl, i.e., the solvent conditions cannot be described as "physiological" either.

Therefore, several intriguing questions remain unanswered. First, whether two or more plateau regions might be possible in the force-extension curves of non-supercoiled dsDNA under physiological solvent conditions? If so, which DNA sequences may be conducive to these highly unusual force-extension curves? Which structural states may be expected? Is the segment order relevant?

To address these questions, one needs to understand the origin of the multi-plateau regime and relate it to the DNA sequence. It is also necessary to characterize structural states that exist in dsDNA in this regime; details of their distributions along the chain are equally important.

Here, we will use a recently proposed approach,[35] coupled with a bead-spring dynamic model of dsDNA/RNA stretching, to predict and explain multiple plateau regions in the force-extension curves of specific dsDNA fragments. We will investigate the multiple plateau regions of the force-extension curves of different DNA fragments, shed light on which structural states exist in dsDNA, and demonstrate their distributions along the dsDNA. We will use the approach to explore the sequence-dependence of dsDNA stretching, as it may show novel, unexpected features. We will propose specific dsDNA fragments likely to exhibit

multi-plateau regions in the future force-extension experiments under physiological solvent conditions at room temperature.

2 Results and discussion

We hypothesize that a dsDNA fragment made up of several segments with distinctly different plateau force values will exhibit multiple plateau regions in the force-extension curve. First, we investigate the possibility of a two-plateau regime. A dsDNA fragment consisting of two segments with two different plateau force values may show two plateau regions in its force-extension curve. If for each segment that constitutes the DNA fragment the plateau region starts approximately at the same values of relative extension, then the segment with a lower plateau force overstretches first (i.e., reaches the plateau region), followed by the overstretching of the segment with a higher plateau force (see, for example, Figure 4).

We then extend the hypothesis to explore the possibility of a three-plateau regime, the corresponding structural states seen along the fragment are also investigated. We also explore whether the order of the distinct DNA segments that make up the whole fragments matters. Finally, the robustness of the predictions to model details is confirmed.

In this work, model polymer chains[35] represent dsDNA fragments that are composed of various combinations of three distinct DNA segments; we vary the specific composition of the chain and the order in which the segments are stitched together along the chain. Each of the segments was previously explored experimentally, and shown to exhibit a typical plateau. The following dsDNA segments are used: (i) dsDNA of alternating A-T sequence (poly(dA-dT) segment) with a plateau force of $\sim$ 35 pN, (ii) dsDNA of alternating G-C sequence (poly(dG-dC) segment) with a plateau force of $\sim$ 75 pN, and (iii) torsionally constrained dsDNA (tcDNA segment) of unknown sequence with a plateau force of $\sim$ 110 pN, see "Methods".

To test our hypothesis computationally, we perform multiple MD simulations that model

the stretching of the following dsDNA fragments: (1) the poly(dA-dT) fragment, (2) the poly(dG-dC) fragment, (3) the poly(dA-dT)-poly(dG-dC) fragment (Figure 1), in which the first half the fragment length is the poly(dA-dT) segment and the other half is the poly(dG-dC) segment, (4) for the poly(dA-dT)-tcDNA-poly(dG-dC) fragment (Figure 2), in which the first ≈ 32.65 percent of the fragment length is the poly(dA-dT) segment, the second ≈ 33.67 percent of the fragment length is the tcDNA segment, and the remaining ≈ 33.67 percent of the fragment length is the poly(dG-dC) segment and (5) dsDNA fragment composed of alternating poly(dA-dT) and poly(dG-dC) segments (alternating (poly(dA-dT)-poly(dG-dC) fragment), Figure 3.

Figure 1: Model polymer chain representing the poly(dA-dT)-poly(dG-dC) fragment made of two distinct segments. The solid vertical line shows the boundary between the poly(dA-dT) and poly(dG-dC) segments. Each dot is a coarse-grained bead, see "Methods".

Figure 2: Model polymer chain representing the poly(dA-dT)-tcDNA-poly(dG-dC) fragment made of three distinct segments. The solid vertical lines show the boundaries between the poly(dA-dT), tcDNA, and poly(dG-dC) segments. Each dot is a coarse-grained bead, see "Methods".

Figure 3: Model polymer chain representing the alternating (poly(dA-dT)-(dG-dC)) fragment. Black and blue dots are coarse-grained beads for the poly(dA-dT) and poly(dG-dC) segments, respectively, see "Methods".

2.1 Two plateau regions

Our MD simulations show that two plateau regions are indeed present in the force-extension curve of the poly(dA-dT)-poly(dG-dC) fragment; this results can be compared to the fa-

miliar one-plateau force-extension curves for the poly(dA-dT) or poly(dG-dC) fragments, (Figure 4). The predicted existence of two plateau regions in the force-extension curve of the poly(dA-dT)-poly(dG-dC) fragment, Figure 4, agrees with experiment,[12] in which two plateau regions were observed in the experimental force-extension curve of λ-phage dsDNA in 5 M betaine[12] (blue symbols, Figure 4). Just as in the experiment, our fragment is made up of two segments with different properties with respect to stretching, which validates our overall approach to constructing sequences that may exhibit multiple plateau regions in the force-extension curve. A fully quantitative agreement with the experiment can not be expected at this point. In the experiment, 5M betaine may enhance the difference between the forces required to overstretch AT-rich and GC-rich regions of the experimental sequences,[12] leading to the observation of two plateau regions in the force-extension curve. In the simulation, the fragment is constructed in a way to make that difference large enough under physiological solvent conditions, to yield two distinct plateau regions in the force-extension curve. In the future, the predicted curve of the fragment should be compared with the experimental one of the same fragment under physiological solvent conditions. To the best of your knowledge, such an experiment has not been reported in the literature.

The distributions (the probability density ρ) of relative bond lengths r/r_0 have two peaks in the first plateau region at $L_x/L_0 \approx 1.275$ and three peaks in the second plateau region at $L_x/L_0 \approx 1.8$, see the insets of Figure 5. In the first plateau region of the force-extension curve ($L_x/L_0 \approx 1.275$), the simulation shows the formation of a macroscopically distinct phase in the poly(dG-dC) segment, but does not exhibit the formation of macroscopically distinct phases in the poly(dA-dT) segment, as illustrated in Figure 6. In the first plateau region at $L_x/L_0 \approx 1.275$, the poly(dA-dT) segment consists of a mix of the two microscopic states: slightly and highly stretched, as shown in Figure 6. In contrast, in the second plateau region at $L_x/L_0 \approx 1.8$, the simulation shows the formation of a macroscopically distinct phase in the poly(dA-dT) segment, but does not show the formation of macroscopically distinct phases in the poly(dG-dC) segment, as illustrated in Figure 6.

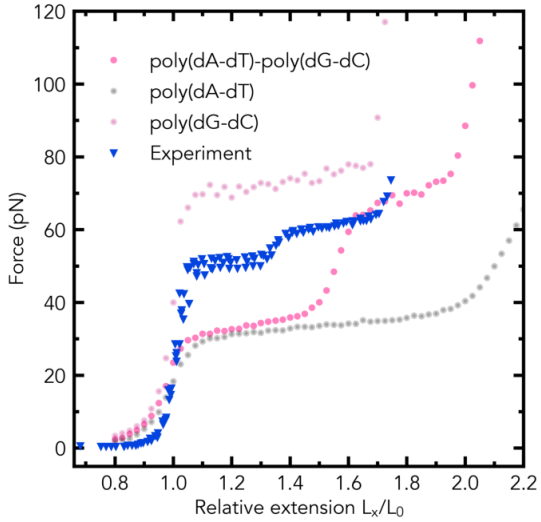

Figure 4: The emergence of two plateau regions in the simulated force-extension curve (pink dots) of a dsDNA fragment made of two segments, Figure 1, with distinctly different plateau force values. Two plateau regions in the force-extension curve are predicted for the poly(dA-dT)-poly(dG-dC) fragment (1078 base pairs in total). Two plateau regions in the experimental force-extension curve are shown for λ-phage dsDNA in 5 M betaine. The experimental data are from Figure 5 of Ref. 12, with the extension values divided by a contour length of 16.4 μm.[12] Single plateau regions in the force-extension curves (simulation) are shown for the poly(dA-dT) and poly(dG-dC) fragments.

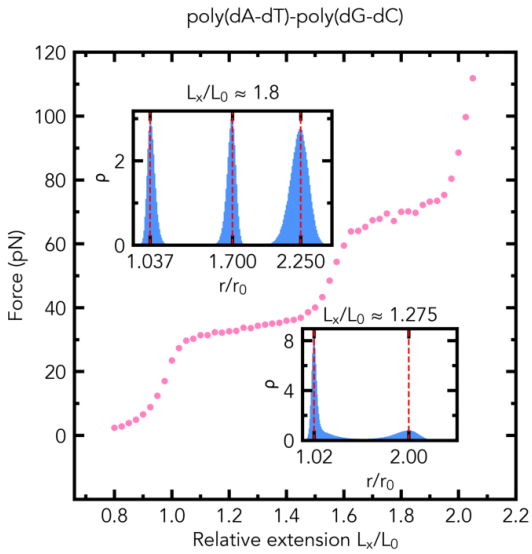

Figure 5: The distributions of states in the plateau regions of the simulated force-extension curve of a dsDNA fragment, Figure 1, made of two segments with distinctly different plateau force values. Two plateau regions in the force-extension curve (pink dots) are predicted for the poly(dA-dT)-poly(dG-dC) fragment (1078 base pairs in total). Insets: The probability density distribution (normalized histogram, n=200) ρ of relative bond lengths r/r_0 at $L_x/L_0 \approx 1.275$ (**Bottom**) and $L_x/L_0 \approx 1.8$ (**Top**).

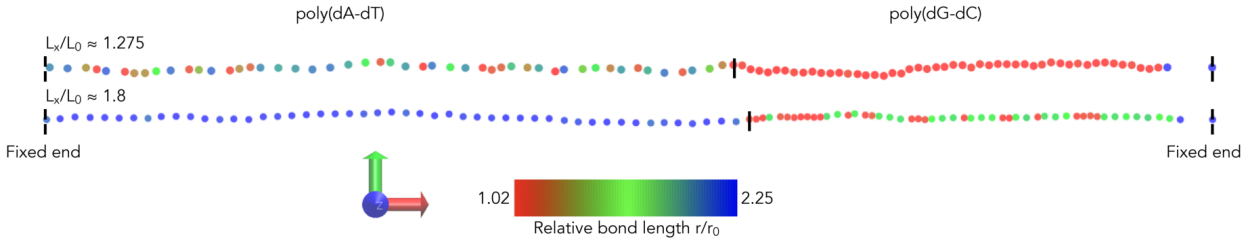

Figure 6: Final equilibrated conformations of the model poly(dA-dT)-poly(dG-dC) fragment in the plateau regions, at two values of the relative extension of the chain (**Top:** $L_x/L_0 \approx 1.275$; **Bottom:** $L_x/L_0 \approx 1.8$). The solid vertical lines show the boundaries between the poly(dA-dT) and poly(dG-dC) segments. The color scale (from red – slight stretching, to blue – high stretching) indicates the relative bond length between the bead of that color and its neighbor to the right.[43]

2.2 Three plateau regions

Our MD simulations reveal that three plateau regions are observed in the force-extension curve of the poly(dA-dT)-tcDNA-poly(dG-dC) fragment (Figure 7). The distributions (the probability density ρ) of relative bond lengths r/r_0 have two peaks in the first plateau region and three peaks in the second and third plateau regions, see the insets of Figure 7. In the first plateau region at $L_x/L_0 \approx 1.175$, the simulation demonstrates the formation of a macroscopically distinct phase in the poly(dG-dC) and tcDNA segments, but does not show the formation of macroscopically distinct phases in the poly(dA-dT) segment, as illustrated in Figure 8. In the first plateau region at $L_x/L_0 \approx 1.175$, the poly(dA-dT) segment consists of a mix of the two microscopic states: slightly and highly stretched, as shown in Figure 8. In contrast, in the second plateau region at $L_x/L_0 \approx 1.525$, the simulation reveals the formation of macroscopically distinct phases in the poly(dA-dT) and tcDNA segments but does not show the formation of macroscopically distinct phases in the poly(dG-dC) segment, as illustrated in Figure 8. In the second plateau region at $L_x/L_0 \approx 1.525$, the poly(dG-dC) segment consists of a mix of the two microscopic states: slightly and highly stretched, as shown in Figure 8. In the third plateau region at $L_x/L_0 \approx 1.85$, the simulation shows the formation of macroscopically distinct phases in the poly(dA-dT) and poly(dG-dC) segments, but does not exhibit the formation of macroscopically distinct phases in the tcDNA segment, as illustrated in Figure 8. In the third plateau region at $L_x/L_0 \approx 1.85$, the tcDNA segment consists of a mix of the two microscopic states: slightly and highly stretched, as shown in Figure 8.

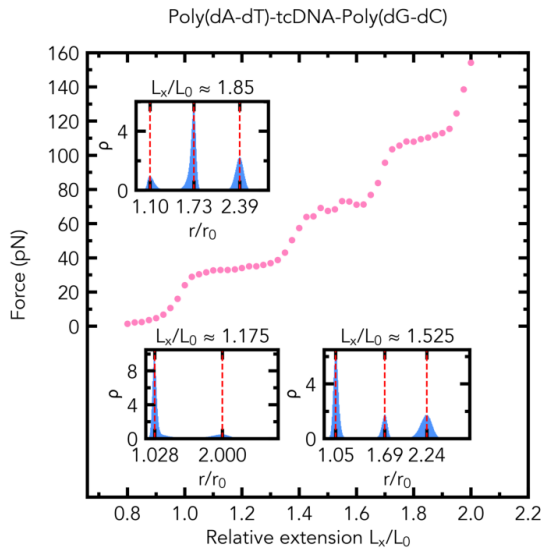

Figure 7: The emergence of three plateau regions in the simulated force-extension curve of a dsDNA fragment made of three segments, Figure 2, with distinctly different plateau force values. Three plateau regions in the force-extension curve are predicted for the poly(dA-dT)-tcDNA-poly(dG-dC) fragment (1078 base pairs in total). The corresponding distributions of states in the plateau regions are shown in the insets. Insets: the probability density (normalized histogram, n=200) ρ of relative bond lengths r/r_0 at $L_x/L_0 \approx 1.175$, $L_x/L_0 \approx 1.525$, and $L_x/L_0 \approx 1.85$.

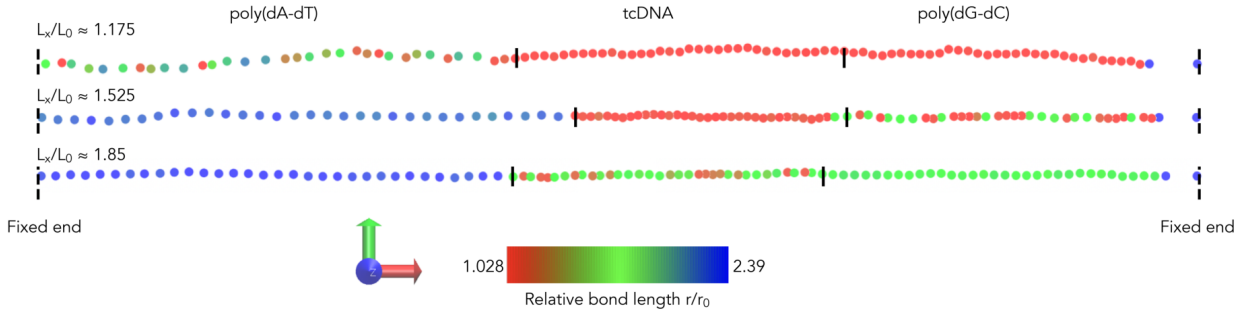

Figure 8: Final equilibrated conformations of the model poly(dA-dT)-tcDNA-poly(dG-dC) fragment in the plateau regions, at three values of the relative extension of the chain (**Top:** $L_x/L_0 \approx 1.175$; **Middle:** $L_x/L_0 \approx 1.525$; **Bottom:** $L_x/L_0 \approx 1.85$). The solid vertical lines show the boundaries between the poly(dA-dT), tcDNA, and poly(dG-dC) segments. The color scale (from red – slight stretching, to blue – high stretching) indicates the relative bond length between the bead of that color and its neighbor to the right.[43]

Another interesting question arises whether the order in which various DNA segments are connected to each other affects the resulting force-extension curves and/or the corresponding distribution of states.

Our MD simulations show that two plateau regions are observed in the force-extension curve of the alternating (poly(dA-dT)-poly(dG-dC)) fragment, Figure 9. As depicted in Figure 5 and Figure 9, the force-extension curve of the alternating (poly(dA-dT)-poly(dG-dC)) fragment is almost the same as that of the poly(dA-dT)-poly(dG-dC) fragment. Therefore, the force-extension curves of the fragments do not depend on the segment order. As in the case of the poly(dA-dT)-poly(dG-dC) fragment, the distributions (the probability density ρ) of relative bond lengths r/r_0 have two peaks in the first plateau region at $L_x/L_0 \approx 1.275$ and three peaks in the second plateau region at $L_x/L_0 \approx 1.8$, see the insets of Figure 9. In the first plateau region at $L_x/L_0 \approx 1.275$, the alternating (poly(dA-dT)-poly(dG-dC)) fragment consists of a mix of the two microscopic states: slightly and highly stretched, whereas, in the second plateau region at $L_x/L_0 \approx 1.8$, the alternating (poly(dA-dT)-poly(dG-dC)) fragment is composed of a mix of the three microscopic states. Therefore, the distribution of states does not change much with the segment order. In the plateau regions of the force-extension curve ($L_x/L_0 \approx 1.275$; $L_x/L_0 \approx 1.8$), the simulations reveal no formation of distinct (macroscopic) phases in the model polymer chain for the alternating (poly(dA-dT)-poly(dG-dC)) fragment.

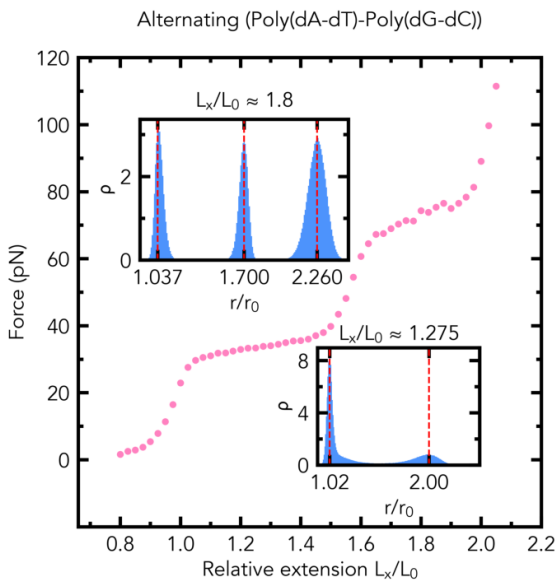

Figure 9: The segment order does not affect the force-extension curve and the distribution of states. Shown are the simulated force-extension curve, and the distribution of states of the alternating (poly(dA-dT)-poly(dG-dC)) fragment (1078 base-pairs in total), made of alternating poly(dA-dT) and poly(dG-dC) segments, Figure 3. The force-extension curve and the distribution of states are almost the same as those of the poly(dA-dT)-poly(dG-dC) fragment, Figure 5. Insets: the probability density (normalized histogram, n=200) ρ of relative bond lengths r/r_0 at $L_x/L_0 \approx 1.275$ and $L_x/L_0 \approx 1.8$.

The approach[35] used here to simulate and describe the complex, multi-plateau force-extension curves of dsDNA fragments, composed of different segments, provides a simple way to rationalize (very few) existing experimental observations and make predictions. Within the approach, for a single plateau force-extension curve of dsDNA, the interplay between the beginning of the plateau region and the stretch modulus of the DNA segment determines the value of the plateau force (height of the plateau). We argue here that the existence of multiple plateau regions in force-extension curves of dsDNA fragment is caused by the mismatch of the plateau force values of its segments.

We argue that combining multiple DNA segments with distinctly different plateau force values leads to multi-plateau force-extension curves and rich distributions of structural states. Within this picture, the DNA sequence affects the existence of multiple plateaux via the distribution of segments along the DNA chain with distinct plateau force values.

2.3 Other predictions and speculations

Besides the dsDNA fragments mentioned above, we also predict that a long dsDNA fragment, composed of the poly(dA-dT), poly(dG-dC), and torsionally unconstrained DNA (see, for example, Figure 3B of Ref. 35; a plateau force of $\sim$ 65 pN) segments might contain three plateau regions in its force-extension curve.

A set of predictions can be made based on the assumption that the stretch modulus of the DNA segment is proportional to its plateau force value. Namely, we predict that the DNA fragment composed of three equal-length segments such as poly(dA-dT), poly(dG-dC), and poly-A[36] and the dsDNA fragment composed of three equal-length segments such as poly(dG-dC), poly-GG,[36] and poly-A[36] might also display three plateau regions in their force-extension curves.

Furthermore, we hypothesize that the existence of the range of forces over which the overstretching transition occurs in λ-phage dsDNA under physiological solvent conditions[12] might be related to the fact that the dsDNA is composed of different segments having variable

force plateau values. When the segments are put together in the dsDNA, then the multiple plateau regions are merged into one plateau region, having a non-zero slope.

3 Conclusions

In this work, we have examined the origin of the multi-plateau region in the force-extension curve of certain non-supercoiled dsDNA fragments, and explored the diverse structural states that arise in these regimes. Employing a bead-spring coarse-grained dynamic model based on a non-convex potential,[35] we predict that a long non-supercoiled double-stranded DNA fragment made up of several segments with different plateau force values for each individual segment will exhibit multiple distinct plateau regions in the force-extension curve under physiological solvent conditions at room temperature. The order of the segments that make up the full DNA fragment does not affect the force-extension curve or the distribution of the corresponding conformational states, at the resolution of the model (one helical turn).

Our MD simulations reveal several specific examples where multi-plateau regions are expected in the force-extension curves of the long DNA fragments under physiologically relevant solvent conditions, such as the poly(dA-dT)-poly(dG-dC) fragment and the poly(dA-dT)-tcDNA-poly(dG-dC) fragment. The formation of mixed states of slightly and highly stretched DNA, co-existing with macroscopically distinct phases in several segments in the plateau regions, is also predicted. The formation of macroscopically distinct phases occurs in those segments that are not within their respective overstretching regions, so no separation into a two-state mixture[35] is expected for those segments in the plateau regions. Our simulations show that the dsDNA fragment consisting of two equal-length segments with two different plateau force values (poly(dA-dT)-poly(dG-dC) fragment) and the DNA fragment consisting of three almost equal-length segments with three different plateau force values (poly(dA-dT)-tcDNA-poly(dG-dC) fragment) displays two plateau regions and three plateau regions in their force-extension curves, respectively. In the case of the stretching

of a long dsDNA fragment consisting of short, alternating poly(dA-dT) and poly(dG-dC) segments (alternating (poly(dA-dT)-poly(dG-dC), equal fraction of each), our model reveals that two plateau regions are observed in the force-extension curve of the polymer without the formation of macroscopically distinct phases in the regions at room temperature. In the future, it will be interesting to explore how the lengths of the plateau regions of the force-extension curves depend on the fractions of the different sequences in the dsDNA fragments.

Our work argues that multiple over-stretching plateaux may be possible to observe under physiologically solvent conditions in non-supercoiled dsDNA – to the best of our knowledge, this prediction is yet to be confirmed experimentally. We have proposed a straightforward criterion for constructing sequences that may lead to these interesting, largely unexplored regimes. We speculate that single-molecule fluorescence resonance energy transfer, with judiciously placed labels, may be used to test the predictions regarding the nature of the structural states that arise in multi-plateau regimes.

Note that all the conclusions above are based on the bead-spring dynamic model,[35] in which the minimum size of the segment is limited to 11 bps; in other words, the resolution of our structural predictions is one helical turn. Other limitations of our approach (model) were discussed in Ref. 35. Despite inevitable limitations of a computational model, we are confident that its qualitative predictions are correct: the existence of a double over-stretching plateau was observed experimentally[12] in a dsDNA fragment made up of two segments with different properties with respect to stretching. In addition, our simulated double plateau force-extension curve of the poly(dA-dT)-poly(dG-dC) fragment qualitatively agrees with a simulated force-extension curve predicted earlier by a multi-state statistical mechanical model for the strongly heterogeneous DNA sequence.[42] We note here a critical advantage of our methodology: it does not assume a certain set of DNA states *a priori*, thus avoiding a potential bias in that respect.

We speculate that the distinct structural states of stretched dsDNA may have functional importance. For example, these can modulate, in a sequence-dependent manner, the rate of

dsDNA processing by key cellular machines.

4 Methods

To perform MD simulation of dsDNA stretching, we use the bead-spring dynamic model and follow the methods described in Ref. 35. The model (approach) reproduced, the experimental stretching behavior of long dsDNA and dsRNA with one plateau region in their force-extension curves.[35] Importantly, the model does not assume any set of structural DNA/RNA states a priori. The model (approach) is based on a theory[25] that links the existence of the plateau region in the force-deformation curve with a non-convex profile of the energy of the system. Specifically, if the energy as a function of deformation is not convex over some interval, then the system minimizes its energy by separating into two states: slightly and highly deformed, with the geometric characteristics of the states corresponding to the beginning and the end of the convex hull of the energy function, respectively.[25,35,44]

All MD simulations are performed in ESPResSo 3.3.1 package[45] with Langevin dynamics at 300 K and an integration time step of 100 fs. Each fragment is represented as a chain of $N = 99$ beads, connected by non-linear springs (non-convex potential). Each bead represents 11 base pairs of DNA ($\sim$ 1 turn of B-DNA), with a diameter and mass of 1 Å and 7150 Da. The parameters of the model for the poly(dA-dT) and poly(dG-dC) segments are shown in Figure 7 of Ref. 35. The parameters of the model for the tcDNA segment are shown in Figure 5A of Ref. 35, except for r_0 which is 37.18 Å, assuming that the helical rise of the tcDNA segment is 3.38 Å. The original experimental force-extension curves of the segments can be found in Figure 5 of Ref. 46, and Figure 9A and B of Ref. 40. In the case of the stretching of the alternating (poly(dA-dT)-poly(dG-dC) fragment, we assume that its persistence length is 95.4 Å. To model long-range interactions explicitly between charged beads in a salt solution, we use the Debye-Hückel potential, whose parameters can be found in Ref. 35. The simulation time is 700 ns, consisting of the 50-ns equilibration run followed

by the 650-ns production run, as in Ref. 35. To check whether 700 ns is a long enough simulation time, we increased the simulation time to 2000 ns for the poly(dA-dT)-poly(dG-dC). Our simulations show that the calculated forces (averaged over 1950 ns) in the plateau regions at $L_x/L_0 \approx 1.275$ ($\sim$ 34.17 pN) and $L_x/L_0 \approx 1.8$ ($\sim$ 73.83 pN) do not differ much from those of the poly(dA-dT)-poly(dG-dC) averaged over 650 ns at $L_x/L_0 \approx 1.275$ ($\sim$ 33.6 pN) and $L_x/L_0 \approx 1.8$ ($\sim$ 70 pN). Other simulation details are provided in the Methods section of Ref. 35 and Table 1 in this work.

Table 1: Simulation details for poly(dA-dT), poly(dG-dC), poly(dA-dT)-poly(dG-dC), alternating (poly(dA-dT)-poly(dG-dC)), and poly(dA-dT)-tcDNA-poly(dG-dC), where γ is the Langevin collision frequency, K_{trap} is the stiffness of the optical trap, and h is the helical rise.

Type	γ^a (ps^{-1})	K_{trap} (k_BT/ Å^2)	h (Å)
poly(dA-dT)	0.0232	6.129	3.38
poly(dG-dC)	0.0327	12.104	3.38
poly(dA-dT)-poly(dG-dC)	0.0232	6.129	3.38
alternating (poly(dA-dT)-poly(dG-dC))	0.0232	6.129	3.38
poly(dA-dT)-tcDNA-poly(dG-dC)	0.0261	7.733	3.38

[a] We deliberately use much smaller values of Langevin γ compared to those of water to dramatically increase the speed of conformational sampling,[47] including the time needed to equilibrate the system. For long DNA fragments, the effective time-scales that can be reached in this low γ regime can be up to 100-fold the nominal trajectory length.[47]

We note that the model already includes the long-range electrostatic interactions implicitly, via its parameters such as the stretch modulus and the persistence length. Furthermore, our previous study[35] demonstrated that the addition of long-range electrostatic interactions explicitly to the model does not affect the distributions of states and the force-extension curves. However, in this work, we decided to repeat the test. To do this, we added the long-range electrostatic interactions, described by the Debye-Hückel potential, to the model. Again, our simulations show that the force-extension curves and the distributions of states do not depend much on the presence of long-range electrostatic interactions.

To check whether the simulation results might depend on the initial conformation of

the model polymer chain, we ran an additional set of simulations from a conformation, in which bond lengths alternate, i.e., slightly and highly stretched. Our simulations show that the force-extension curves and the distributions of states do not depend much on the initial conformation of the model polymer chain.

In Figure 6, the simulations start from the "one-phase" conformations, in which the beads are equally spaced with $r/r_0 = 1.275$ (top) and $r/r_0 = 1.8$ (bottom). In Figure 8, the simulations start from the "one-phase" conformations, in which the beads are equally spaced with $r/r_0 = 1.175$ (top), $r/r_0 = 1.525$ (middle), and $r/r_0 = 1.85$ (bottom).

Acknowledgement

This work was supported in part by the National Institutes of Health, grant R01 GM144596.

References

(1) Ma, J.; Bai, L.; Wang, M. D. Transcription Under Torsion. *Science* **2013**, *340*, 1580–1583.

(2) Burnham, D. R.; Kose, H. B.; Hoyle, R. B.; Yardimci, H. The mechanism of DNA unwinding by the eukaryotic replicative helicase. *Nature Communications* **2019**, *10*.

(3) Hall, M. A.; Shundrovsky, A.; Bai, L.; Fulbright, R. M.; Lis, J. T.; Wang, M. D. High-resolution dynamic mapping of histone-DNA interactions in a nucleosome. *Nature Structural & Molecular Biology* **2009**, *16*, 124–129.

(4) Marin-Gonzalez, A.; Vilhena, J. G.; Perez, R.; Moreno-Herrero, F. A molecular view of DNA flexibility. *Quarterly Reviews of Biophysics* **2021**, *54*.

(5) Lionnet, T.; Dawid, A.; Bigot, S.; Barre, F.-X.; Saleh, O. A.; Heslot, F.; Allemand, J.-F.; Bensimon, D.; Croquette, V. DNA mechanics as a tool to probe helicase and translocase activity. *Nucleic Acids Research* **2006**, *34*, 4232–4244.

(6) Basu, A.; Bobrovnikov, D. G.; Ha, T. DNA mechanics and its biological impact. *Journal of Molecular Biology* **2021**, *433*, 166861.

(7) Wasserman, M. R.; Liu, S. A Tour de Force on the Double Helix: Exploiting DNA Mechanics To Study DNA-Based Molecular Machines. *Biochemistry* **2019**, *58*, 4667–4676.

(8) Lipfert, J.; Skinner, G. M.; Keegstra, J. M.; Hensgens, T.; Jager, T.; Dulin, D.; Kober, M.; Yu, Z.; Donkers, S. P.; Chou, F.-C.; Das, R.; Dekker, N. H. Double-stranded RNA under force and torque: Similarities to and striking differences from

double-stranded DNA. *Proceedings of the National Academy of Sciences* **2014**, *111*, 15408–15413.

(9) Herrero-Galán, E.; Fuentes-Perez, M. E.; Carrasco, C.; Valpuesta, J. M.; Carrascosa, J. L.; Moreno-Herrero, F.; Arias-Gonzalez, J. R. Mechanical Identities of RNA and DNA Double Helices Unveiled at the Single-Molecule Level. *Journal of the American Chemical Society* **2013**, *135*, 122–131, PMID: 23214411.

(10) Fu, H.; Zhang, C.; Qiang, X.-W.; Yang, Y.-J.; Dai, L.; Tan, Z.-J.; Zhang, X.-H. Opposite Effects of High-Valent Cations on the Elasticities of DNA and RNA Duplexes Revealed by Magnetic Tweezers. *Physical Review Letters* **2020**, *124*, 058101, PRL.

(11) Yeou, S.; Lee, N. K. Single-Molecule Methods for Investigating the Double-Stranded DNA Bendability. *Molecules and cells* **2022**, *45*, 33–40.

(12) Smith, S. B.; Cui, Y.; Bustamante, C. Overstretching B-DNA: The Elastic Response of Individual Double-Stranded and Single-Stranded DNA Molecules. *Science* **1996**, *271*, 795–799.

(13) van Mameren, J.; Gross, P.; Farge, G.; Hooijman, P.; Modesti, M.; Falkenberg, M.; Wuite, G. J. L.; Peterman, E. J. G. Unraveling the structure of DNA during overstretching by using multicolor, single-molecule fluorescence imaging. *Proceedings of the National Academy of Sciences* **2009**, *106*, 18231–18236.

(14) Paik, D. H.; Perkins, T. T. Overstretching DNA at 65 pN Does Not Require Peeling from Free Ends or Nicks. *Journal of the American Chemical Society* **2011**, *133*, 3219–3221, PMID: 21207940.

(15) Cizeau, P.; Viovy, J.-L. Modeling extreme extension of DNA. *Biopolymers* **1997**, *42*, 383–385.

(16) Ahsan, A.; Rudnick, J.; Bruinsma, R. Elasticity Theory of the B-DNA to S-DNA Transition. *Biophysical Journal* **1998**, *74*, 132–137.

(17) Storm, C.; Nelson, P. C. Theory of high-force DNA stretching and overstretching. *Physical Review E* **2003**, *67*.

(18) Léger, J. F.; Romano, G.; Sarkar, A.; Robert, J.; Bourdieu, L.; Chatenay, D.; Marko, J. F. Structural Transitions of a Twisted and Stretched DNA Molecule. *Physical Review Letters* **1999**, *83*, 1066–1069.

(19) Marko, J. F. DNA under high tension: Overstretching, undertwisting, and relaxation dynamics. *Phys. Rev. E* **1998**, *57*, 2134–2149.

(20) Haijun, Z.; Yang, Z.; Zhong-can, O.-Y. Bending and Base-Stacking Interactions in Double-Stranded DNA. *Physical Review Letters* **1999**, *82*, 4560–4563.

(21) Rief, M.; Fernandez, J. M.; Gaub, H. E. Elastically Coupled Two-Level Systems as a Model for Biopolymer Extensibility. *Physical Review Letters* **1998**, *81*, 4764–4767.

(22) Argudo, D.; Purohit, P. K. Equilibrium and Kinetics of DNA Overstretching Modeled with a Quartic Energy Landscape. *Biophysical Journal* **2014**, *107*, 2151–2163.

(23) Rouzina, I.; Bloomfield, V. A. Force-Induced Melting of the DNA Double Helix 1. Thermodynamic Analysis. *Biophysical Journal* **2001**, *80*, 882–893.

(24) Sarkar, A.; Léger, J.-F.; Chatenay, D.; Marko, J. F. Structural transitions in DNA driven by external force and torque. *Physical Review E* **2001**, *63*.

(25) Savin, A. V.; Kikot, I. P.; Mazo, M. A.; Onufriev, A. V. Two-phase stretching of molecular chains. *Proceedings of the National Academy of Sciences* **2013**, *110*, 2816–2821.

(26) Romano, F.; Chakraborty, D.; Doye, J. P. K.; Ouldridge, T. E.; Louis, A. A. Coarse-grained simulations of DNA overstretching. *The Journal of Chemical Physics* **2013**, *138*, 085101.

(27) Luan, B.; Aksimentiev, A. Strain Softening in Stretched DNA. *Phys. Rev. Lett.* **2008**, *101*, 118101.

(28) Fiasconaro, A.; Falo, F. Dynamical model for the full stretching curve of DNA. *Phys. Rev. E* **2012**, *86*, 032902.

(29) Šulc, P.; Romano, F.; Ouldridge, T. E.; Doye, J. P. K.; Louis, A. A. A nucleotide-level coarse-grained model of RNA. *The Journal of Chemical Physics* **2014**, *140*, 235102.

(30) Pupo, A. E. B.; Falo, F.; Fiasconaro, A. DNA overstretching transition induced by melting in a dynamical mesoscopic model. *The Journal of Chemical Physics* **2013**, *139*, 095101.

(31) Cluzel, P.; Lebrun, A.; Heller, C.; Lavery, R.; Viovy, J.-L.; Chatenay, D.; Caron, F. DNA: An Extensible Molecule. *Science* **1996**, *271*, 792–794.

(32) Lebrun, A.; Lavery, R. Modelling Extreme Stretching of DNA. *Nucleic Acids Research* **1996**, *24*, 2260–2267.

(33) Li, H.; Gisler, T. Overstretching of a 30 bp DNA duplex studied with steered molecular dynamics simulation: Effects of structural defects on structure and force-extension relation. *The European Physical Journal E* **2009**, *30*.

(34) Wolter, M.; Elstner, M.; Kubař, T. On the Structure and Stretching of Microhydrated DNA. *The Journal of Physical Chemistry A* **2011**, *115*, 11238–11247.

(35) Afanasyev, A. Y.; Onufriev, A. V. Stretching of Long Double-Stranded DNA and RNA Described by the Same Approach. *Journal of Chemical Theory and Computation* **2022**, *18*, 3911–3920.

(36) Marin-Gonzalez, A.; Vilhena, J. G.; Moreno-Herrero, F.; Perez, R. Sequence-dependent mechanical properties of double-stranded RNA. *Nanoscale* **2019**, *11*, 21471–21478.

(37) Marin-Gonzalez, A.; Vilhena, J.; Moreno-Herrero, F.; Perez, R. DNA Crookedness Regulates DNA Mechanical Properties at Short Length Scales. *Physical Review Letters* **2019**, *122*.

(38) Lankaš, F.; Šponer, J.; Hobza, P.; Langowski, J. Sequence-dependent elastic properties of DNA. *Journal of Molecular Biology* **2000**, *299*, 695–709.

(39) Lankaš, F. DNA sequence-dependent deformability-insights from computer simulations. *Biopolymers* **2004**, *73*, 327–339.

(40) Clausen-Schaumann, H.; Rief, M.; Tolksdorf, C.; Gaub, H. E. Mechanical Stability of Single DNA Molecules. *Biophysical Journal* **2000**, *78*, 1997–2007.

(41) Bustamante, C.; Bryant, Z.; Smith, S. B. Ten years of tension: single-molecule DNA mechanics. *Nature* **2003**, *421*, 423–427.

(42) Whitelam, S.; Pronk, S.; Geissler, P. L. Stretching chimeric DNA: A test for the putative S-form. *The Journal of Chemical Physics* **2008**, *129*, 205101.

(43) Humphrey, W.; Dalke, A.; Schulten, K. VMD: Visual molecular dynamics. *Journal of Molecular Graphics* **1996**, *14*, 33–38.

(44) Drozdetski, A. V.; Mukhopadhyay, A.; Onufriev, A. V. Strongly Bent Double-Stranded DNA: Reconciling Theory and Experiment. *Frontiers in Physics* **2019**, *7*, 195.

(45) Limbach, H.; Arnold, A.; Mann, B.; Holm, C. ESPResSo—an extensible simulation package for research on soft matter systems. *Computer Physics Communications* **2006**, *174*, 704–727.

(46) King, G. A.; Burla, F.; Peterman, E. J. G.; Wuite, G. J. L. Supercoiling DNA optically. *Proceedings of the National Academy of Sciences* **2019**, *116*, 26534–26539.

(47) Anandakrishnan, R.; Drozdetski, A.; Walker, R.; Onufriev, A. Speed of Conformational Change: Comparing Explicit and Implicit Solvent Molecular Dynamics Simulations. *Biophysical Journal* **2015**, *108*, 1153–1164.